

FREQUENCY RESPONSE ANALYSIS OF HYBRID PIEZOELECTRIC CANTILEVER BEAM

Petr Sadílek*, Robert Zemčík*

Frequency response analysis of hybrid aluminium beam with piezoelectric actuators was performed using finite element method. The finite element model was implemented in Matlab software. The one-dimensional beam element is based on Euler-Bernoulli theory and it assumes bilinear distribution of electric field potential. The piezoelectric actuators were driven by harmonic signals around the first eigenfrequency and the beam oscillations were investigated. Results were compared to experiment.

Keywords: *piezo, finite element, hybrid, beam, modal analysis*

1. Introduction

As the demands on the ratio of stiffness and strength to weight of structures are rising, light-weight structures are nowadays necessary components in modern state-of-the-art products in all sorts of industries. One of the solutions is usage of composite materials. Composite materials are mostly man-made materials made from one or more hard non-continuous component materials imbedded in a less hard continuous material with significantly different physical or chemical properties. The connection creates a new structure. The physical properties of the new structure are generally not isotropic, but rather are typically orthotropic and therefore can be altered according to the assumed type and direction of loading unlike the isotropic materials.

The increasing requirements on structural performance call for the usage of embedded sensors and actuators, resulting in the construction of so-called smart or adaptive structures that can thus respond to loading conditions in real time. One type of smart materials are piezoelectric materials. The piezoelectric effect describes the relation between mechanical stress and electrical voltage in solids. It is reversible: applied mechanical stress will generate voltage and applied voltage will change the shape of the solid by a small amount. This enables for instance to suppress vibrations or to move amplitudes out of the range of eigenfrequencies, provided that proper electronic control circuits are applied.

The first experimental demonstration of a connection between macroscopic piezoelectric phenomena and crystallographic structure was published in 1880 by Pierre and Jacques Curie. The converse piezoelectric effect was mathematically deduced by Lippmann in 1881. The first finite element implementation of the piezoelectric phenomenon came in 1970 by Allik and Hughes [1]. After that, many researches equipped the standard structural finite elements with the piezoelectric capability to simulate the piezoelectric effect. To simulate

* Ing. P. Sadílek, Ing. R. Zemčík, Ph.D., Faculty of Applied Sciences, UWB in Pilsen, Univerzitní 22, 306 14 Plzeň, Czech Republic

it, the similarity to the theory of thermo-elasticity was sometimes used. These early models concerned mainly 3D-solid elements, which are not suited for efficient analysis of laminated shell structures. For this reason, the approach changed and in the recent years, the piezoelectric, beam, plate and shell elements are used more frequently. Cen et al. [3], for example, developed a four-node plate element for laminated structures based on first-order shear deformation theory while Lee et al. [7] introduced a nine-node assumed strain element allowing variable thickness, which is not possible for other elements. Hybrid laminated piezo plates are studied by Mitchell and Reddy [11] using higher-order shear deformation theory and layerwise approach for electric potential. Dynamic behavior of smart laminated plates using the layerwise approach are studied by Saravanas et al. [12]. Tzou et al. [14] investigate the control of smart conical shells using triangular finite elements. Kögl and Bucalem [6] introduced a MITC based element suitable for modelling of moderately thick sandwich smart structures. They stress the importance of quadratic variation of electric potential across the layer thickness to accurately model the electric field. There are more various finite element approaches summarized for example in the survey by Benjeddou [2]. Piefort and Preumont [8,9] use piezoelectric materials for sensing and actuation in vibration and vibroacoustic control of plates modelled by Mindlin shell elements. Zhou et al. [15] study free vibrations of piezoelectric bimorphs by means of analytical solution. Heyliger [4] and later Heyliger and Wu [5] present exact analytical solution for laminated piezoelectric cylinder and sphere, respectively. Zemčík et al. [17] developed four-noded piezoelectric shell element and implemented into commercial code ANSYS.

The element proposed in this paper is two-noded and has two structural degrees of freedom (DOFs) at each node plus two DOFs for electric potential. Elements are considered as beams. The piezoelectric coupling is full and direct (i.e. non-iterative), and it is intended for the simulation of applied piezoelectric layers – patches.

Presented work is developed for testing purposes. Goal of the future work is to design and perform structural health monitoring of composite structures with piezoelectric components for the identification of damage of the structure. Hybrid (piezoelectric) elements are not commonly available in existing commercial software. They are defined mainly as solid elements, whereas shell, beam, and namely layered elements, are very sporadic.

2. Mathematical model

2.1. Constitutive equations

The theory of piezoelectric materials used here assumes symmetrical hexagonal piezoelectric structure – class 6mm (C_{6v}). Only the laminar piezoelectric effect (so-called d_{31} effect [13]) is considered, i.e., the material is polarized in the thickness direction.

The pure mechanical stress-strain law for each piezoelectric element is extended with piezoelectric coupling [16]. This can be than rewritten as

$$\begin{aligned}\boldsymbol{\sigma} &= \mathbf{C}\boldsymbol{\varepsilon} - \mathbf{e}^T \mathbf{E} , \\ \mathbf{D} &= \mathbf{e}\boldsymbol{\varepsilon} + \boldsymbol{\epsilon} \mathbf{E} ,\end{aligned}\tag{1}$$

where \mathbf{D} is the vector of electric flux density, $\boldsymbol{\epsilon}$ is the dielectric permittivity matrix, \mathbf{e} is the piezoelectric coefficient matrix and \mathbf{E} is the electric field vector.

The first of the two equations above is the well-known Hooke's relation between stress and strain extended by piezoelectric coupling.

The permittivity matrix ϵ is defined as

$$\epsilon = \begin{bmatrix} \epsilon_{11} & 0 & 0 \\ 0 & \epsilon_{22} & 0 \\ 0 & 0 & \epsilon_{33} \end{bmatrix} \quad (2)$$

and the piezoelectric matrix \mathbf{e} as

$$\mathbf{e} = \begin{bmatrix} 0 & 0 & 0 & 0 & e_{15} & 0 \\ 0 & 0 & 0 & e_{24} & 0 & 0 \\ e_{31} & e_{32} & e_{33} & 0 & 0 & 0 \end{bmatrix}. \quad (3)$$

2.2. Analytical formulation

The beam element is based on Euler-Bernoulli theory. It has two nodes with one deflection w_n and one rotational φ_n DOF at each node (see Fig. 1). Let the deflection $w(x)$ across the length be approximated by the polynomial:

$$w(x) = a_0 + a_1 x + a_2 x^2 + a_3 x^3 = \mathbf{N} \mathbf{w}, \quad (4)$$

where \mathbf{N} is matrix of approximation functions and the structural DOF vector is ordered as

$$\mathbf{w} = [w_n, \varphi_n, w_{n+1}, \varphi_{n+1}]^T. \quad (5)$$

Then, the axial displacement can be written as

$$u(x, z) = z \varphi(x) = z \frac{\partial w}{\partial x} \quad (6)$$

and, consequently, the axial strain is

$$\varepsilon(x, z) = \frac{\partial u}{\partial x} = z \frac{\partial^2 w}{\partial x^2} = \mathbf{B} \mathbf{w}, \quad (7)$$

where \mathbf{B} is strain-displacement matrix consisting of shape functions derivatives.

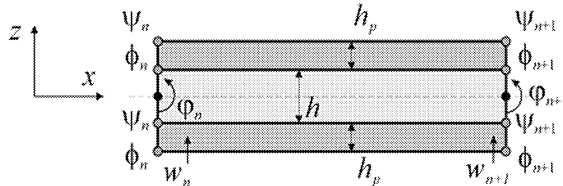


Fig.1: Element geometry example; piezo material (dark grey) and its supporting structure (light grey) sharing common nodes (degrees of freedom)

Similarly, let the electric field potential $\phi(x, z)$ be approximated by bi-linear function

$$\phi(x, z) = a_4 + a_5 x + a_6 z + a_7 x z. \quad (8)$$

Hence, the electric field intensity vector \mathbf{E} is

$$\mathbf{E} = -\nabla\phi = \mathbf{\Phi} \phi , \quad (9)$$

where $\mathbf{\Phi}$ is the electric field intensity-potential matrix and the electrical DOF vector is ordered as

$$\phi = [\phi_n, \psi_n, \phi_{n+1}, \psi_{n+1}]^T \quad (10)$$

with ϕ_n and ψ_n being the potential values on the lower and upper surfaces, respectively (see Fig. 1).

2.3. Variational principle

The equations of motion of a piezoelectric structure can be derived from the Lagrangian and the virtual work which must include both the mechanical and the electrical contributions. The potential energy density P of a piezoelectric material includes contributions from the strain energy and from the electrostatic energy, hence [2]

$$P = \frac{1}{2} \boldsymbol{\sigma}^T \boldsymbol{\varepsilon} - \frac{1}{2} \mathbf{D}^T \mathbf{E} = \frac{1}{2} \boldsymbol{\varepsilon}^T \mathbf{C} \boldsymbol{\varepsilon} - \mathbf{E}^T \mathbf{e} \boldsymbol{\varepsilon} - \frac{1}{2} \mathbf{E}^T \boldsymbol{\varepsilon} \mathbf{E} \quad (11)$$

while the kinetic energy density is simply

$$K = \frac{1}{2} \rho (\dot{w})^2 . \quad (12)$$

Let us confine to case without external mechanical forces and electric charge. The Lagrangian can then be written in the form

$$L = \int_V (K - P) dV . \quad (13)$$

Using the variation principle, the condition

$$\delta L = 0 \quad (14)$$

must be satisfied for any arbitrary variation of the displacements and electrical potentials, thus the resulting equations of motion with the assumptions made above are assembled as

$$\begin{bmatrix} \mathbf{M}_{uu} & \mathbf{0} \\ \mathbf{0} & \mathbf{0} \end{bmatrix} \begin{bmatrix} \ddot{\mathbf{w}} \\ \dot{\boldsymbol{\phi}} \end{bmatrix} + \begin{bmatrix} \mathbf{K}_{uu} & \mathbf{K}_{u\phi} \\ \mathbf{K}_{u\phi}^T & \mathbf{K}_{\phi\phi} \end{bmatrix} \begin{bmatrix} \mathbf{w} \\ \boldsymbol{\phi} \end{bmatrix} = \begin{bmatrix} \mathbf{0} \\ \mathbf{0} \end{bmatrix} , \quad (15)$$

where the submatrices (element stiffness, piezoelectric coupling, capacitance and mass matrix) are

$$\begin{aligned} \mathbf{K}_{uu} &= \int_V \mathbf{B}^T \mathbf{C} \mathbf{B} dV & [4 \times 4] , \\ \mathbf{K}_{u\phi} &= - \int_V \mathbf{B}^T \mathbf{e} \mathbf{\Phi} dV & [4 \times 4] , \\ \mathbf{K}_{\phi\phi} &= - \int_V \mathbf{\Phi}^T \boldsymbol{\varepsilon} \mathbf{\Phi} dV & [4 \times 4] , \\ \mathbf{M}_{uu} &= \rho \int_V \mathbf{N}^T \mathbf{N} dV & [4 \times 4] . \end{aligned} \quad (16)$$

For a case with external mechanical forces and electric charge the equation changes to

$$\begin{bmatrix} \mathbf{M}_{uu} & \mathbf{0} \\ \mathbf{0} & \mathbf{0} \end{bmatrix} + \begin{bmatrix} \ddot{\mathbf{w}} \\ \ddot{\boldsymbol{\phi}} \end{bmatrix} + \begin{bmatrix} \mathbf{K}_{uu} & \mathbf{K}_{u\phi} \\ \mathbf{K}_{u\phi}^T & \mathbf{K}_{\phi\phi} \end{bmatrix} \begin{bmatrix} \mathbf{w} \\ \boldsymbol{\phi} \end{bmatrix} = \begin{bmatrix} \mathbf{F} \\ \mathbf{Q} \end{bmatrix}, \quad (17)$$

where the right-hand side vector consists of a vector of nodal forces \mathbf{F} and of a vector of electrode electric charges \mathbf{Q} .

2.4. Modal analysis

In order to perform the modal analysis the system must be statically condensed. By expanding (15), two equations can be obtained in the following manner:

$$\mathbf{M}_{uu} \ddot{\mathbf{w}} + \mathbf{K}_{uu} \mathbf{w} + \mathbf{K}_{u\phi} \boldsymbol{\phi} = \mathbf{0}, \quad (18)$$

$$\mathbf{K}_{u\phi}^T \mathbf{w} + \mathbf{K}_{\phi\phi} \boldsymbol{\phi} = \mathbf{0}. \quad (19)$$

From (19) we can express $\boldsymbol{\phi}$ as

$$\boldsymbol{\phi} = -\mathbf{K}_{\phi\phi}^{-1} \mathbf{K}_{u\phi}^T \mathbf{w}. \quad (20)$$

Inserting (20) into (18) and by simplifying following equation is obtained:

$$\mathbf{M}_{uu} \ddot{\mathbf{w}} + \left(\mathbf{K}_{uu} - \mathbf{K}_{u\phi} \mathbf{K}_{\phi\phi}^{-1} \mathbf{K}_{u\phi}^T \right) \mathbf{w} = \mathbf{0} \quad (21)$$

and the problem reduces to the eigenvalue analysis of the matrix

$$\mathbf{A} = \mathbf{M}_{uu}^{-1} \left(\mathbf{K}_{uu} - \mathbf{K}_{u\phi} \mathbf{K}_{\phi\phi}^{-1} \mathbf{K}_{u\phi}^T \right). \quad (22)$$

The corresponding values for electrical DOFs can be retrieved using (20). The set of equations in (15) for single element is expanded accordingly in finite element analysis when joining element with common nodes (see Fig. 1).

2.5. Static analysis

Let us consider that there are no mechanical forces and no inertia forces applied on the beam. Then (15) changes to

$$\begin{bmatrix} \mathbf{K}_{uu} & \mathbf{K}_{u\phi} \\ \mathbf{K}_{u\phi}^T & \mathbf{K}_{\phi\phi} \end{bmatrix} \begin{bmatrix} \mathbf{w} \\ \boldsymbol{\phi} \end{bmatrix} = \begin{bmatrix} \mathbf{0} \\ \mathbf{0} \end{bmatrix}, \quad (23)$$

and the displacements can be expressed as

$$\mathbf{w} = \mathbf{K}_{uu}^{-1} \mathbf{K}_{u\phi} \boldsymbol{\phi}. \quad (24)$$

When deflections are known then according to (15) again we can also compute the charges by solving

$$\mathbf{Q} = \mathbf{K}_{u\phi}^T \mathbf{w} + \mathbf{K}_{\phi\phi} \boldsymbol{\phi}. \quad (25)$$

3. Experiment

An experiment was carried out [10] with an aluminium beam and two collocated piezoelectric patches with properties in Tab.1. The patches (DuraAct P876.A12, operating voltage -100 to 400 V) were glued to the skins using HBM Z70 glue. The beam was clamped on one end (see Fig. 2) with total length $l_b = 500$ mm, width $b_b = 30$ mm and thickness $h_b = 3$ mm. The dimensions of the piezopatches were length $l = 61$ mm, width $b = 35$ mm and thickness $h = 0.3$ mm. From the total length of the piezopatch only 50 mm may be considered as active. The patches were loaded by an electric signal

$$\phi = \Phi \sin(\omega t) ,$$

where Φ is voltage amplitude.

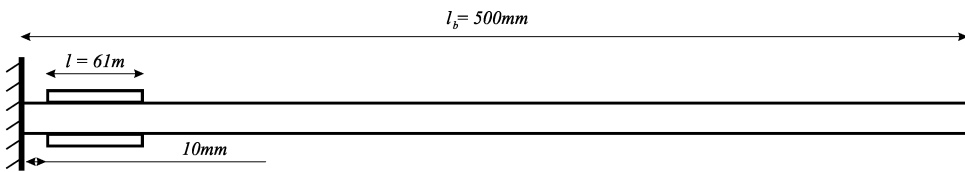


Fig.2: Schema of location of piezopatches on the beam

This caused deformation of the piezo actuators and consequently this induced oscillation of the free end. Deflection magnitude was measured through a laser equipment (Fig. 3). Plundrich [10] compared his results with finite elements method in MSC.Marc, where he used solid elements for beam and the patches in structured mesh. He simulated piezoelectric effect through similarity with thermal expansion. He was also searching for eigenfrequencies. The two lowest eigenfrequencies measured were $f_1 = 9.5$ Hz and $f_2 = 59$ Hz.

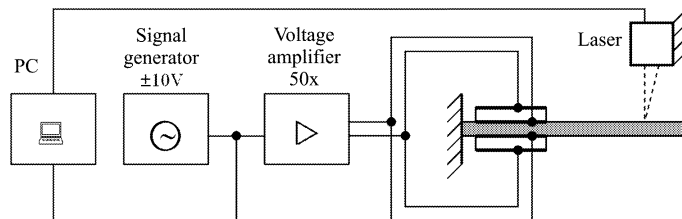


Fig.3: Diagram of experiment arrangement

Property	E [GPa]	μ [-]	ρ [kg/m ³]	e_{31} [Cm ⁻²]
Aluminium	70.0	0.33	2670	—
Piezo	61.8	0.30	7760	5.6

Tab.1: Properties of used materials

4. Numerical tests

Three types of analyses were carried out using Matlab code. The first one included static loading of the beam to find out the deflection of the free end.

Using constant voltage $\phi = 0.7\text{ V}$ in (24) amplified 50 times resulted in deflection (see Fig. 4) of the free end

$$u = 6.6 \times 10^{-5}\text{ m} \tag{27}$$

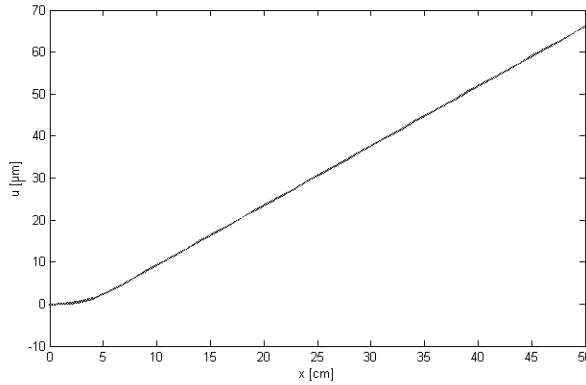


Fig.4: Deflection of a beam made of 50 elements with static loading

The second was the modal analysis. The two lowest eigenfrequencies found were $f_1 = 9.9256\text{ Hz}$ and $f_2 = 62.2024\text{ Hz}$. Higher frequencies were not searched for.

Thirdly, knowing the eigenvalues, the analysis focused on comparison to experiment and results from MSC.Marc. The numerical model of the beam was loaded by waveforms close to first eigenfrequency. Central differences in the time domain were used in the Matlab model. Material damping was not included as it is more complicated and difficult to reach convergence. Comparison to experiment and results from MSC.Marc can be found in Tab. 2 and Tab. 3. Voltage differs because of experimental apparatus setting. Absence of damping caused higher amplitudes for Matlab model. For graphical interpretation see Fig. 5.

Frequency [Hz]	0.97	1.95	2.81	4.02	4.88	5.85	6.96	7.93	8.67	9.76	10.74
Voltage Φ [V]	35.0	42.5	31.0	43.5	41.0	43.5	40.5	34.5	35.5	41.5	36.5
Experiment	0.10	0.10	0.11	0.13	0.16	0.17	0.19	0.21	0.30	5.5	0.41
MSC.Marc	0.06	0.07	0.05	0.09	0.09	0.11	0.13	0.16	0.22	0.64	1.31
Matlab	0.07	0.10	0.08	0.14	0.15	0.20	0.24	0.30	0.43	1.40	1.00

Tab.2: Comparison of aluminium beam amplitudes [mm] induced by harmonic waveform (part 1)

Frequency [Hz]	11.59	12.45	13.55	14.52	15.62	16.60	17.70	18.43	19.77
Voltage Φ [V]	33.5	29.0	30.0	40.5	32.0	29.0	33.5	33.0	38.0
Experiment	0.28	0.18	0.12	0.10	0.07	0.06	0.05	0.04	0.06
MSC.Marc	0.29	0.14	0.09	0.09	0.05	0.04	0.04	0.04	0.39
Matlab	0.64	0.32	0.22	0.22	0.14	0.11	0.11	0.10	0.10

Tab.3: Comparison of aluminium beam amplitudes [mm] induced by harmonic waveform (part 2)

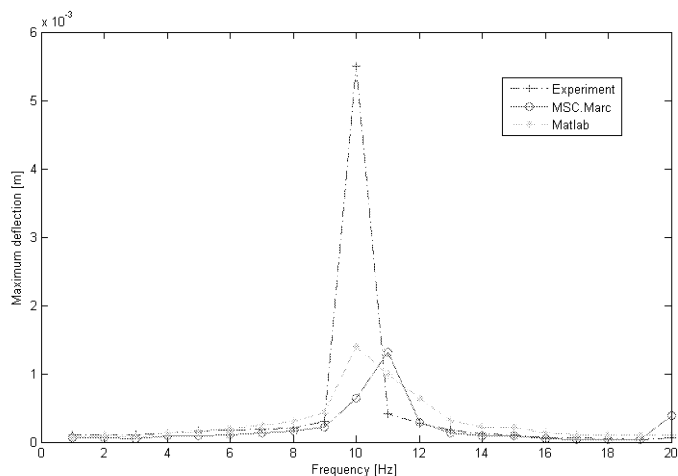


Fig.5: Graphical comparison of amplitudes induced by harmonic loading

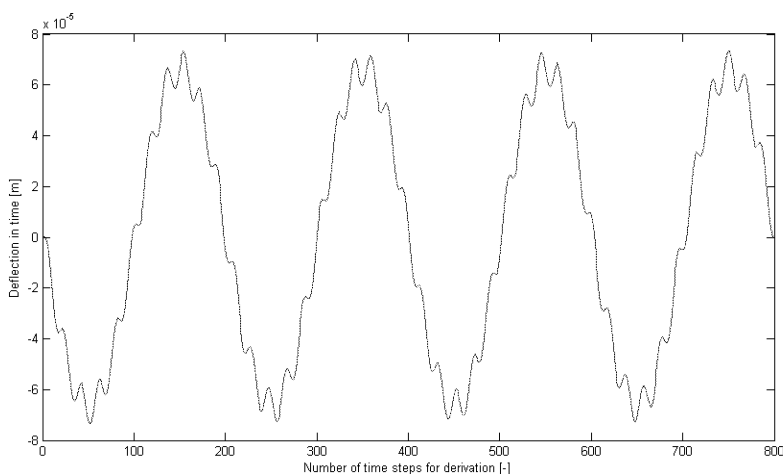


Fig.6: Free end oscillation through time for frequency 0.97 Hz

5. Conclusion

The presented work is focused on application of piezoelectric materials on composite structures. The approach deals with finite element method. One dimensional beam element suitable for the analysis of structures with applied piezoelectric sensors and actuators, i.e. smart structures, is developed and implemented in Matlab code. The element is based on Euler-Bernoulli theory and it assumes bilinear distribution of electric field potential. Static and modal analyses were carried out to verify convergence of a simple beam model. The model was consequently loaded with harmonic waveforms and compared to experiment. The discrepancy between results was low. Numerical model did not include material damping but the results were closer to experiment than the results from MSC.Marc.

As only the essential research on finite element model was made, further investigation is necessary. Future work will be among other things focused on the influence of the material damping mentioned. Numerical tests with material damping were already performed, but did not show convergence. The cause will be investigated.

Upon the study of the state-of-the-art it shows, that piezoelectric materials may be well adapted for industrial structure health monitoring (SHM) systems. One of the main advantages of SHM is, that it can reveal damage that may have occurred between scheduled intervals of inspections. Also the inspection is only visual, therefore forms of damage such as delamination of composites can be easily overlooked. With help of SHM system using piezoelectric sensors it is thus possible to detect and identify also hidden defects in real time.

Therefore the forthcoming steps of future work is to investigate possibilities of piezoelectric materials. Optimal location for piezopatches for investigation of eigenfrequencies will be searched for. In further work experimental comparison of two bodies will be undertaken, where the second body will represent the first object with an artificial defect. Through combination of finite element method and optimization methods the research will focus on identifying the range and position of the defect.

Acknowledgements

The work has been supported by the research project MSM 4977751303 and project of Grant Agency of the Czech Republic 101/08/P091.

References

- [1] Allik H., Hughes T.J.R.: Finite element method for piezoelectric vibration, *International Journal for Numerical Methods in Engineering*, 2, pp. 151–157, 1970
- [2] Benjeddou A.: Advances in piezoelectric finite element modeling of adaptive structural elements: a survey, *Computers and Structures*, 76, pp. 347–363, 2000
- [3] Cen S., Soh A.-K., Long Y.-Q., Yao Z.-H.: A new 4-node quadrilateral FE model with variable electrical degrees of freedom for the analysis of piezoelectric laminated composite plates, *Composite Structures*, 58, pp. 583–599, 2002
- [4] Heyliger P.: A note on the static behavior of simply supported laminated piezoelectric cylinders, *Int. J. Solids Structures*, 34, No. 29, pp. 3781–3794, 1997
- [5] Heyliger P., Wu Y.-C.: Electroelastic fields in layered piezoelectric spheres, *International Journal of Engineering Science*, 37, pp. 143–161, 1999
- [6] Kögl M., Bucalem M.L.: Analysis of smart laminates using piezoelectric MITC plate and shell elements, *Computers and Structures*, 83, pp. 1153–1163, 2005
- [7] Lee S., Goo N., Park H.C., Yoon K.J., Cho C.: A nine-node assumed strain shell element for analysis of a coupled electro-mechanical system, *Smart Mater. Struct.*, 12, pp. 355–362, 2003
- [8] Piefort V.: Finite Element Modelling of Piezoelectric Active Structures, PhD Thesis, ULB, Bruxelles, 2001
- [9] Piefort V., Preumont A.: Finite element modelling of smart piezoelectric shell structures, 5th National Congress on Theoretical and Applied Mechanics, Louvain-la-Neuve, 2000
- [10] Plundrich T.: Analýza kompozitového nosníku s aktivními prvky, Master thesis, University of West Bohemia, Plzen, 2008
- [11] Reddy J.N.: An evaluation of equivalent single-layer and layerwise theories of composite laminates, *Composite Structures*, 25, pp. 31–35, 1993
- [12] Saravanan D.A., Heyliger P.R., Hopkins D.A.: Layerwise mechanics and finite element for the dynamic analysis of piezoelectric composite plates, *Int. J. Solids Structures*, 34, No. 3, pp. 359–378, 1997
- [13] Tzou H.S.: Piezoelectric shells, Distributed sensing and control of continua, Kluwer Academic Publishers, 1993
- [14] Tzou H.S., Wang D.W., Chai W.K.: Dynamics and distributed control of conical shells laminated with full and diagonal actuators, *Journal of Sound and Vibration*, 256(1), pp. 65–79, 2002

- [15] Zhou Y., Chen Y., Ding H.: Analytical modelling and free vibration analysis of piezoelectric bimorphs, *Journal of Zhejiang University Science*, 6A(9), pp. 938–944, 2005
- [16] Zemčík R.: Non-stationary progressive failure analysis of fiber-reinforced composites, Doctoral thesis, Univeristy of West Bohemia, Plzeň, 2005
- [17] Zemčík R., Rolfes R., Rose M., Tessler J.: High-performance four-node shell element with piezoelectric coupling for the analysis of smart laminated structures, *Int. J. Numer. Meth. Engng.*, 70, pp. 934–961, 2007

Received in editor's office: June 4, 2009

Approved for publishing: June 1, 2010